Enzyme and Microbial Technology 78 (2015) 40–45

Contents lists available at ScienceDirect

Enzyme and Microbial Technology

journal homepage: www.elsevier.com/locate/emt

Glucose biosensor based on glucose oxidase immobilized at gold nanoparticles decorated graphene-carbon nanotubes

Rajkumar Devasenathipathy[a], Veerappan Mani[a,b], Shen-Ming Chen[a,*], Sheng-Tung Huang[a,b,**], Tsung-Tao Huang[b,c], Chun-Mao Lin[d], Kuo-Yuan Hwa[e], Ting-Yo Chen[a,b], Bo-Jun Chen[a,b]

[a] Department of Chemical Engineering and Biotechnology, National Taipei University of Technology, No.1, Section 3, Chung-Hsiao East Road, Taipei 106, Taiwan
[b] Institute of Biochemical and Biomedical Engineering, National Taipei University of Technology, No.1, Section 3, Chung-Hsiao East Road, Taipei 106, Taiwan
[c] Biomedical Instrument Technology Division, Instrument Technology Research Center, National Applied Research Laboratories, 20, R&D Rd. VI, Hsinchu Science Park, Hsinchu, Taiwan
[d] Department of Biochemistry, College of Medicine, Taipei Medical University, No. 250, Wu-xing Street, Taipei 110, Taiwan
[e] Department of Molecular Science and Engineering, National Taipei University of Technology, Taipei, Taiwan

ARTICLE INFO

Article history:
Received 16 April 2015
Received in revised form 8 June 2015
Accepted 9 June 2015
Available online 18 June 2015

Keywords:
Graphene
Carbon nanotubes
Gold nanoparticles
Glucose oxidase
Biosensor
Electrochemistry

ABSTRACT

Biopolymer pectin stabilized gold nanoparticles were prepared at graphene and multiwalled carbon nanotubes (GR-MWNTs/AuNPs) and employed for the determination of glucose. The formation of GR-MWNTs/AuNPs was confirmed by scanning electron microscopy, X-ray diffraction, UV–vis and FTIR spectroscopy methods. Glucose oxidase (GOx) was successfully immobilized on GR-MWNTs/AuNPs film and direct electron transfer of GOx was investigated. GOx exhibits highly enhanced redox peaks with formal potential of −0.40 V (vs. Ag/AgCl). The amount of electroactive GOx and electron transfer rate constant were found to be 10.5×10^{-10} mol cm^{-2} and 3.36 s^{-1}, respectively, which were significantly larger than the previous reports. The fabricated amperometric glucose biosensor sensitively detects glucose and showed two linear ranges: (1) 10 μM – 2 mM with LOD of 4.1 μM, (2) 2 mM – 5.2 mM with LOD of 0.95 mM. The comparison of the biosensor performance with reported sensors reveals the significant improvement in overall sensor performance. Moreover, the biosensor exhibited appreciable stability, repeatability, reproducibility and practicality. The other advantages of the fabricated biosensor are simple and green fabrication approach, roughed and stable electrode surface, fast in sensing and highly reproducible.

1. Introduction

The development of efficient glucose biosensors for the sensitive determination of blood glucose level is significantly important [1,2]. Electrochemical biosensors are the most preferable methods for the determination of blood glucose due to their simplicity, sensitivity, portability, and direct use in point-of-care assays [3,4]. Glucose oxidase (GOx) is the model enzyme employed for the enzymatic determination of glucose [5]. However, there are two important limitations in immobilizing GOx on solid electrodes: (1) poor electrical communication between active site of GOx and electrode surface, and (2) enzyme leaching [6,7]. The preparation of suitable electrode matrix is significantly important to overcome these issues [3,7]. Nonetheless, the electrode matrix should not alter the mechanical stability and catalytic ability of GOx [4,8]. A wide variety of electrode materials including polymers [9], sol-gel [10], mesoporous silica [11], metal nanoparticles [12], carbon nanotubes [13] and graphene based nanomaterials [14,15] have been reported in the past years. Recently, carbon nanomaterials such as multiwalled carbon nanotubes (MWNTs) and graphene (GR) are proved as promising electrode materials for fabrication of electrochemical biosensors attributed to their large surface area, high conductivity, and good catalytic ability [8]. Designing GR based nanocomposites for the development of glucose biosensors is continuous research interest in our research group [3,6,8,16–18]. Herein, we described a simple electrochemical approach for the preparation of gold nanoparticles (AuNPs) at pectin scaffold and

* Corresponding author. Fax: + 886 2270 25238.
** Corresponding author. Fax: +886 02 2731 7117.
E-mail addresses: smchen78@ms15.hinet.net (S.-M. Chen), ws75624@ntut.edu.tw (S.-T. Huang).

http://dx.doi.org/10.1016/j.enzmictec.2015.06.006
0141-0229/

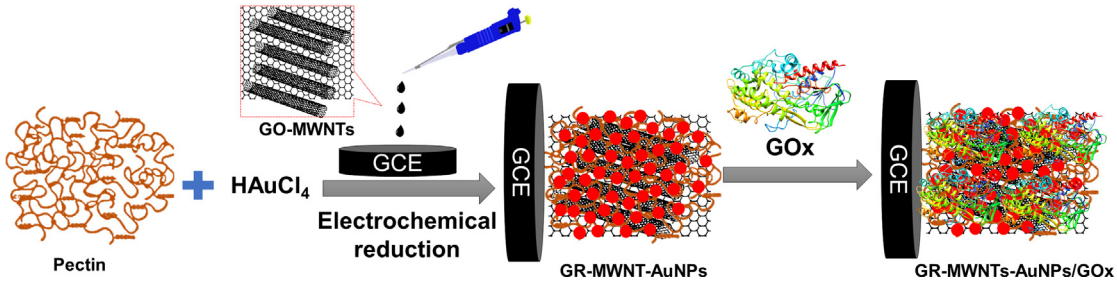

Scheme 1. Schematic representation for the fabrication of GR-MWNTs/AuNPs/GOx film modified GCE.

GR-MWNTs (GR-MWNTs/AuNPs). MWNTs own high mechanical strength, excellent conductivity, antifouling properties and shown great glucose sensing ability [8]. Green agents stabilized AuNPs have been widely used for the fabrication of biosensors ascribed to their long-term stability, solubility, less toxicity and amphiphilicity.

The main aim of this work is to develop a sensitive glucose biosensor based on GR-MWNTs/AuNPs. The GR-MWNTs/AuNPs was prepared through easily adoptable electrodeposition method. The GR-MWNTs/AuNPs/GOx film exhibits excellent electrocatalytic ability for the determination of glucose and displayed wide linear range, low limit of detection and high sensitivity. The glucose biosensing performance of the GR-MWNTs/AuNPs/GOx is quite comparable to the previously reported glucose biosensors. The other advantages of the biosensor are simple and green fabrication approach, roughed and stable electrode surface, fast in sensing and highly reproducible.

2. Experimental

2.1. Chemicals and apparatus

Graphite (powder, <20 μm), MWNTs (bundled > 95%, O.D × I.D × length of 7–15 nm × 3–6 nm × 0.5–200 μm), pectin (from citrus peel), $HAuCl_4$, GOx (type *x–s*, *Aspergillus niger*) and all the other reagents were purchased from Sigma-Aldrich and used as received. All the electrochemical measurements were carried out using CHI 611A electrochemical work station (CH Instruments, Inc., U.S.A) at ambient temperature. Electrochemical studies were performed in a conventional three electrode cell using modified glassy carbon electrode (GCE) (Bioanalytical Systems, Inc., USA) as a working electrode (area 0.071 cm^2), saturated Ag|AgCl (saturated KCl) as a reference electrode and Pt wire as a counter electrode. Prior to each electrochemical experiment, the electrolyte solutions were deoxygenated with pre-purified nitrogen for 15 min unless otherwise specified. The supporting electrolyte used for the electrochemical studies was 0.1 M phosphate buffer (pH 7) prepared from sodium dihydrogen phosphate and disodium hydrogen phosphate. To perform different pH study, 0.1 M acetate buffer from acetic acid and sodium acetate (for pH 3 and 5), and 0.1 M Tris-buffered saline (TBS) from tris and sodium chloride (for pH 9) were prepared.

Amperometric measurements were performed with analytical rotator AFMSRX (PINE instruments, USA) with a rotating disc electrode (RDE) having working area of 0.21 cm^2. Scanning electron microscopy (SEM) and UV–vis absorption spectroscopic measurements were performed using Hitachi S-3000H scanning electron microscope and Hitachi U-3300 spectrophotometer (EquipNet, Inc., USA). Powder X-ray diffraction (XRD) and Attenuated total reflectance-FT-IR (ATR–FTIR) spectroscopy studies were carried out using XPERT-PRO (PANalytical B.V., The Netherlands) diffractometer (Cu Kα radiation, $k = 1.54$ Å) and Perkin-Elmer IR spectrometer respectively.

2.2. Synthesis of GR-MWNTs/AuNPs and immobilization of GOx

Graphite oxide was prepared from graphite by Hummers method [19] and exfoliated to graphene oxide (GO) via ultrasonic agitation. 10 mg MWNTs were added in 5 mL of GO (1 mg mL^{-1}) and ultrasonicated for 2 h to get GO-MWNTs [20]: The composite was washed (water and ethanol), dried and redispersed in water (0.5 mg mL^{-1}). GCE surface was cleaned by polishing with 0.05 μm alumina slurry using Buehler polishing kit. 5 μL GO-MWNTs was drop cast on the pre-cleaned GCE and dried at ambient conditions. Subsequently, GO-MWNTs modified electrode was transferred to an electrochemical cell containing 5 mL of KNO_3 (0.1 M) with pectin (3 mg mL^{-1}) and $HAuCl_4$ (0.3 mg mL^{-1}). 10 consecutive cyclic voltammograms were swept at a scan rate of 50 mV s^{-1}. The potential range was + 1.40 V to −1.40 V [21]. During electrochemical cycling, GO was reduced to GR [3]. Simultaneously, pectin stabilized Au^{3+} ions were reduced and electrodeposited on GR-MWNTs. The as-prepared GR-MWNTs/AuNPs film was rinsed with water and dried. 5 μL GOx (10 mg mL^{-1}) was drop cast onto GR-MWNTs/AuNPs film and dried at room temperature (Scheme 1). GR-MWNTs/AuNPs/GOx film modified electrode was gently washed with water and dried. As control, AuNPs/GOx, MWNTs/AuNP/GOx and GR/AuNPs/GOx electrodes were prepared.

3. Results and discussion

3.1. Characterization of GR-MWNTs/AuNPs

SEM image of GR portrays characteristic wrinkled thin sheet like morphology with foldings and crumbles (Fig. S1A). The SEM image of GR-MWNTs shows thin GR sheets along with tubular networks of MWNTs (Fig. S1B) [22]. The SEM image of GR-MWNTs/AuNPs (Fig. 1A) depicts uniform decoration of pectin stabilized AuNP at GR-MWNTs. The particle sizes are ranging between 15 nm and 70 nm. Fig. 1B displays UV–Vis spectra of pectin (curve a) and GR-MWNTs/AuNPs (**curve b**). The spectrum of pectin presents a sharp absorption peak at 291 nm and a shoulder at 380 nm which were arose due to the presence of free carboxyl group. However, these absorption peaks were disappeared in the spectrum of GR-MWNTs/AuNPs indicating that these free carboxyl groups are committed to accommodate AuNPs. At the same time, a new absorption peak was observed at 562 nm which is assigned to the AuNPs. ATR–FTIR spectrum of pectin (**curve a,** Fig. 1C) shows well-defined peaks at the wavenumbers of 3615, 2980, 1789 and 1616 cm^{-1} corresponding to —OH, $—CH_3$, $—COOCH_3$ and C=O functionalities, respectively. However, all these peaks were disappeared in the spectrum of GR-MWNTs/AuNPs (**curve b,** Fig. 1C) indicating the removal of oxygen functionalities during reduction. The obser-

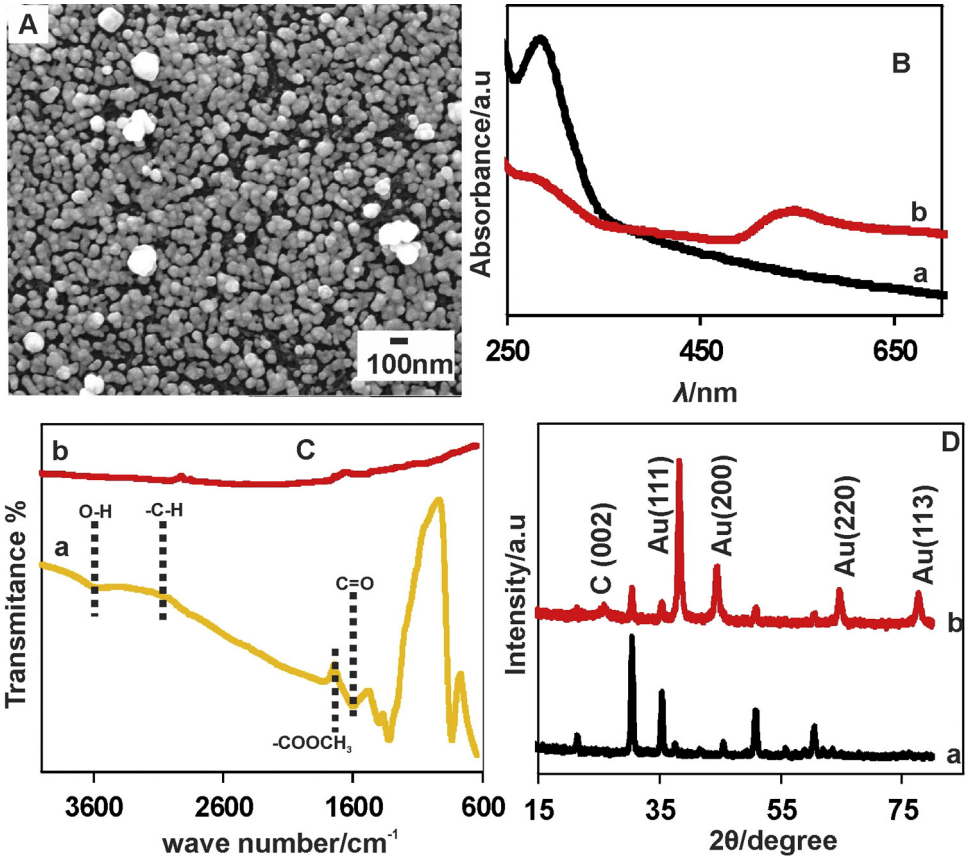

Fig. 1. (A) SEM image of GR-MWNTs/AuNPs; UV–vis (B) and ATR–FTIR (C) spectra of pectin (a) and GR-MWNTs/AuNPs (b); (D) XRD patterns of bare ITO (a) and GR-MWNTs/AuNPs (b).

vation of four diffraction peaks at 2θ angles of 38.3°, 44.46°, 64.78° and 77.96° were assigned to (1 1 1), (2 0 0), (2 2 0) and (3 1 1) reflections of face-centered cubic structure of AuNPs, respectively (JCPDS, card no. 04-0784) (Fig. 1D) [23].

3.2. Direct electron transfer of GOx

Fig. 2**A** presents the cyclic voltammograms of AuNPs/GOx (a) MWNTs/AuNPs/GOx (b), GR/AuNPs/GOx (c), GR-MWNTs/GOx (d) and GR-MWNTs/ AuNPs/GOx (e) films modified GCEs in phosphate buffer (pH 7) at the scan rate of 50 mVs^{-1}. The AuNPs/GOx film has not exhibited any redox peaks indicating its impotence to mediate the direct electron transfer of GOx. The redox peaks of GOx observed at all other electrodes denote direct electron transfer of FAD/$FADH_2$. Electrochemical parameters of the redox couple, such as formal potential ($E^{\circ\prime}$), anodic peak current density (j_{pa}), cathodic peak current density (j_{pc}), and peak potential separation value (ΔE_p) are given in Table S1. The direct electron transfer ability of these modified electrodes follows; MWNTs/AuNPs/GOx< GR/AuNPs/GOx< GR-MWNTs/GOx< GR-MWNTs/AuNPs/GOx. GR-MWNTs/AuNPs/GOx film exhibits maximum direct electron transfer ability than other electrodes which is evident from its low ΔE_p and greatly enhanced peak currents (j_{pa} and j_{pc}). The excellent electron transfer ability of the film should be attributed to its large surface area, high conductivity, high porosity and biocompatibility. GR-MWNTs possess high edge density due to its three dimensional hierarchical network which provides large surface area and high conductivity. In addition, there is good synergy between GR and MWNTs. The GR-MWNTs/GOx exhibits comparatively less electron transfer ability than the GR-MWNTs/AuNPs/GOx which revealed the significant contribution of AuNPs to improve the direct electron transfer ability. 200 consecutive CVs are carried out in phosphate buffer (pH 7) in order to investigate stability of GR-MWNTs/AuNPs/GOx film modified electrode; The electrode was retained 96.16% of its initial response currents (I_{pa} and I_{pc}) even after 200 successive cycles (Fig. S2). Besides, the electrode was retained 95.74% of its initial peak currents (I_{pa} and I_{pc}) even after one month storage time indicating the good stability of the developed modified electrode.

Fig. 2B presents cyclic voltammograms of GR-MWNTs/AuNPs/GOx in phosphate buffer (pH 7) at different scan rates (100 to 1000 $mV\,s^{-1}$). Both I_{pa} and I_{pc} of the redox couple increases as scan rates increases (ν). A plot of I_{pa} and I_{pc} vs. ν exhibits good linearity with slope of 277.2 μA. $(Vs^{-1})^{-1}$ and −280.5 μA. $(Vs^{-1})^{-1}$ respectively, indicating surface confined process (inset to Fig. 2B). The surface coverage of GOx (Γ) at GR-MWNTs/AuNPs film was calculated using Eq. (1) [24].

$$I_p = \frac{n^2F^2\nu A\Gamma}{4RT} \quad (1)$$

Here, ν (Vs^{-1}), A (cm^2) and n (=2) are referring scan rate, electrode surface area and number of electrons transferred. The constants R, T and F are representing their usual meanings ($R = 8.314\,J\,K^{-1}\,mol^{-1}$, $T = 298\,K$, $F = 96485C\,mol^{-1}$). The value of Γ is calculated to be 1.05×10^{-9} mol cm^{-2} which is significantly higher than previously reported electrodes; reduced GO-MWNTs (3.58×10^{-10} mol cm^{-2}) [3], GR-cobalt phthalocyanines (3.77×10^{-10} mol cm^{-2}) [16] and reduced GO (1.22×10^{-10} mol cm^{-2}) [6]. The apparent heterogeneous electron transfer rate constant (k_s) of GOx at GR-MWNTs/AuNPs film was calculated using Eq. (2) (where,

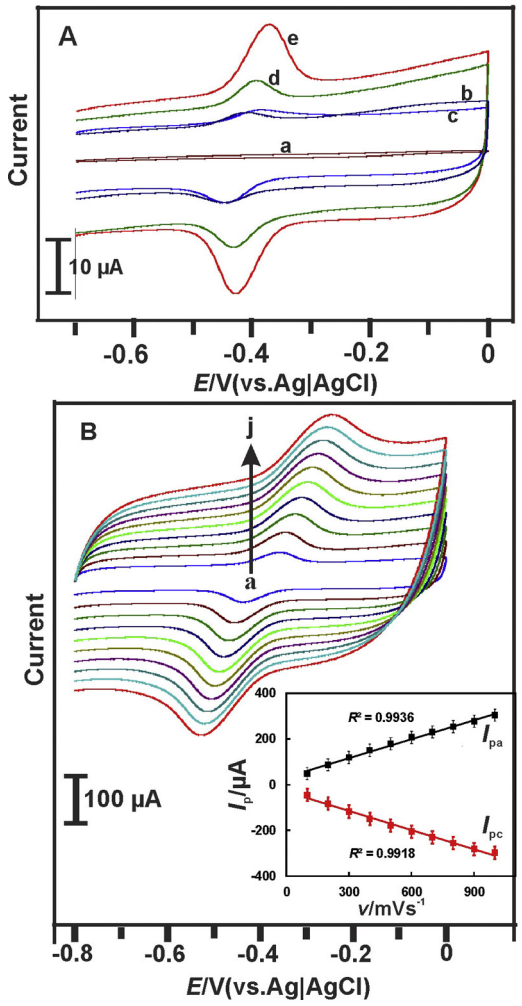

Fig. 2. (A) Cyclic voltammograms obtained at AuNPs/GOx (a) MWNTs/AuNPs/GOx (b) GR/AuNPs/GOx (c), GR-MWNTs/GOx (d) and GR-MWNTs/AuNPs/GOx (e) films modified GCE in phosphate buffer (pH 7) at the scan rate of 50 mV s^{-1}. (B) Cyclic voltammograms obtained at GR-MWNTs/AuNPs/GOx in phosphate buffer (pH 7) at different scan rates (100–1000 mV s^{-1}). Inset: Plot of I_{pa} and I_{pc} vs. ν, I_{pa}/μA = 277.2 ν/Vs^{-1} −33.81/μA; I_{pc}/μA = −280.5 ν/Vs^{-1} −30.23/μA.

$\Delta E_p \geq 100$ mV) [24],

$$\text{Log}k_s = \alpha\log(1-\alpha) + (1-\alpha)\log\alpha - \log(RT/nF\nu) - \alpha(1-\alpha)nF\Delta E_p/2.3RT \quad (2)$$

here, α is the charge transfer coefficient (≈0.5), while all other parameters stands for similar meanings explained in Eq. (1). The value of k_s is calculated to be 3.36 s^{-1}, which is significantly greater than those reported for GOx immobilized on boron-doped CNTs (1.56 s^{-1}) [25], GOx–GR–chitosan (2.83 s^{-1}) [26], gelatin–MWNTs (1.08 s^{-1}) [8], CNTs-gold colloid (1.01 s^{-1}) [27], MWNTs-chitosan (1.08 s^{-1}) [28], and single-walled CNTs-chitosan modified electrode (3.0 s^{-1}) [29].

Effect of electrolyte pH on the direct electron transfer of GOx was investigated in different pH ranging from 3 to 9 (Fig. 3A). Despite GOx presents sharp redox peaks in all pH, it has the tendency to denature at low and high pH values [30]. At pH 7, GOx exhibits maximum redox peak currents. The plot between $E^{\circ\prime}$ and pH exhibits good linearity (Fig. 3B) with slope of −52 mV/pH. The slope value is close to the theoretical value of − 58.6 mV/pH accounted for a reversible reaction involving equal numbers of protons and electrons [3].

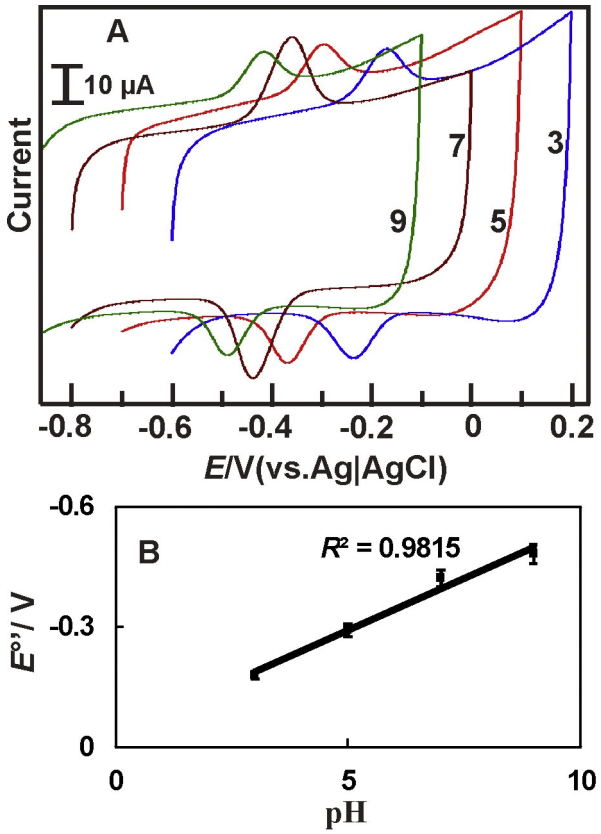

Fig. 3. (A) Cyclic voltammograms obtained at GR-MWNTs/AuNPs/GOx film modified electrode in phosphate buffer with different pH ranging from 3 to 9. (B) Plot of $E^{\circ\prime}$ vs. pH; $E^{\circ\prime}$/V = −52 (mV/pH) −0.0331.

3.3. Electrocatalysis and determination of glucose

Fig. S3 displays the cyclic voltammograms of GR-MWNTs/AuNPs/GOx film modified GCE in nitrogen (a), air (b) and oxygen (c) saturated phosphate buffer (pH 7). In the oxygen saturated condition, the electrode presents a sharp increase in the j_{pc} which should be ascribed to the excellent oxygen reduction reaction (ORR) ability of the electrode. Fig. 4A presents the voltammograms of GR-MWNTs/AuNPs/GOx in oxygen saturated phosphate buffer (pH 7) containing different concentration of glucose. A sharp decrease in j_{pc} was observed upon injection of glucose which is due to the consumption of oxygen required for GOx catalyzed oxidation of glucose [3]. The concentration of glucose dependent linear plot displays good linearity in the concentration range of 1–7 mM (Fig. 4B).

Fig. 5A displays the amperogram of GR-MWNTs/AuNPs/GOx film modified RDE for various concentration of glucose (10,100 and 1000 μM). Aliquots of glucose were injected at 50 s regular intervals into continuously stirred phosphate buffer (pH 7). The applied electrode potential (E_{app}) was hold at −0.44 V, while rotation speed was fixed at 1500 rpm. Rapid and well defined responses were observed for each addition. The amperometric responses are linearly increased in the concentration range of 10 μM–2 mM (Fig. 5B). A plot between [glucose] and I_p exhibits good linearity with slope of 0.146 μA mM^{-1}. Sensitivity of the biosensor was calculated to be 0.695 μA mM^{-1} cm^{-2}, while detection limit was calculated as 4.1 μM (S/N=3). A second linear range was observed in the concentration range of 2–5.2 mM with slope of 0.050 μA mM^{-1} (Fig. 5C). Sensitivity and detection limit at this linear range were 0.2380 μAmM^{-1} cm^{-2} and 0.95 mM respectively. The important analytical parameters such as detection limit, linear range and sen-

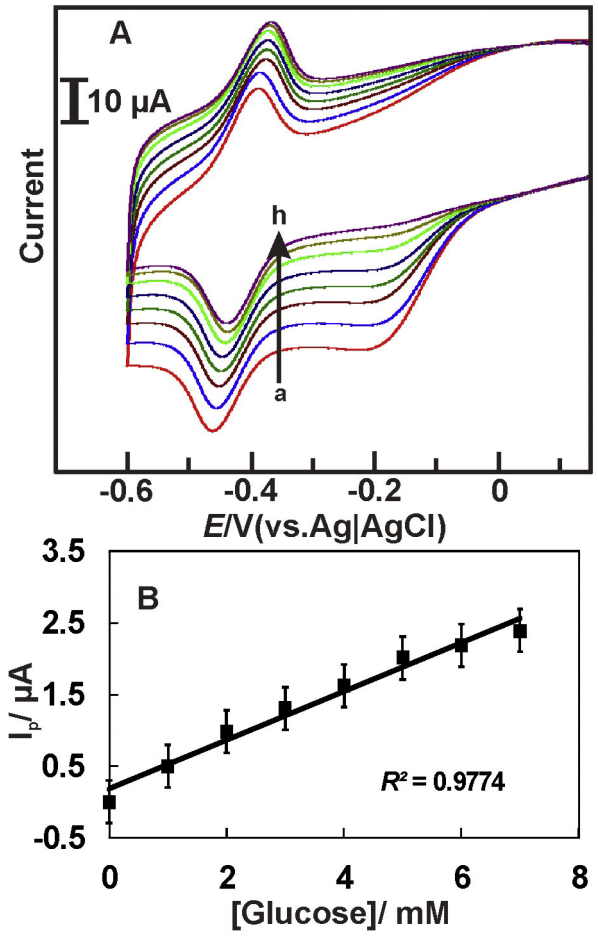

Fig. 4. (A) Cyclic voltammograms obtained at GR-MWNTs/AuNPs/GOx film in oxygen saturated phosphate buffer (pH 7) in the absence (a) and presence of glucose (b to h; each addition of 1 mM glucose). (B) Plot of I_p vs. [glucose]; $I_p/\mu A = 0.341$ [glucose]/μA mM^{-1} + 0.1825.

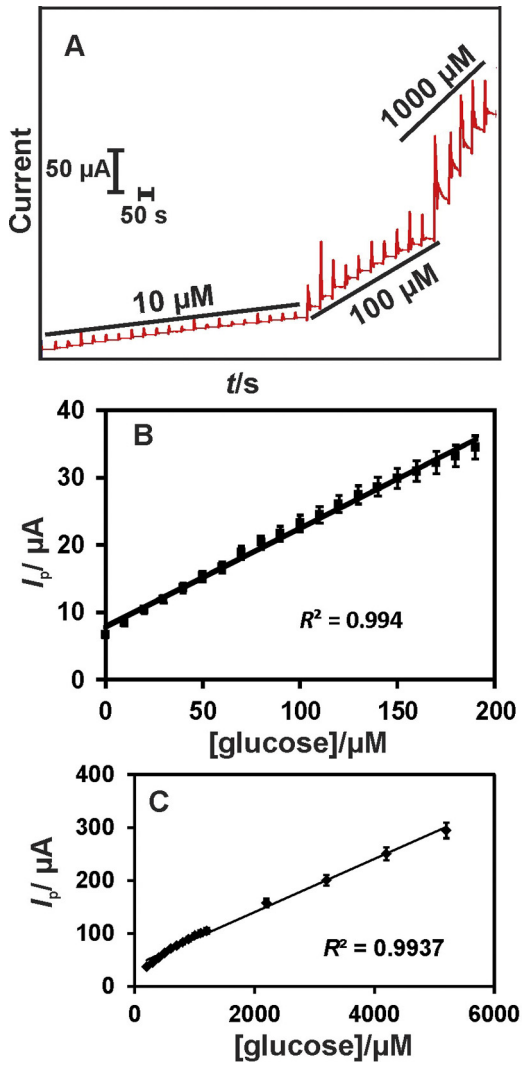

Fig. 5. (A) Amperometric response obtained at GR-MWNTs/AuNPs/GOx electrode for successive addition of glucose (10 μM, 100 μM and 1 mM) into continuously stirred oxygen saturated phosphate buffer (pH 7). E_{app} = –0.44 V, Rotation rate = 1500 rpm (B) Plot of I_p vs [glucose]; $I_p/\mu A = 0.146$ [glucose]/μA M^{-1} + 7.78. (C) Plot of I_p vs. [glucose]; $I_p/\mu A = 0.050$ [glucose]/μA mM^{-1} + 39.69.

sitivity were compared with reported glucose biosensors (Table S2). As seen from the table, the described film exhibited significantly improved sensing ability than the previously reported carbon nanomaterials based glucose biosensors.

3.4. Stability, repeatability, reproducibility and practicality

To investigate storage stability of the biosensor, its response current to detect glucose (3 mM) was monitored every day. The biosensor was retained 94.37% of its initial response current even after two months storage period which indicates its good storage stability. The electrode was stored at 4 °C when not in use. Only 5.3% of the initial response current (to detect 3 mM glucose) was loosed even after 300 successive scans, revealing the excellent stability of the sensor. The biosensor exhibits good repeatability (seven repeated measurements) and reproducibility (seven individual measurements) with an R.S.D of 1.86% and 2.37%, respectively.

Practical feasibility of the biosensor has been assessed in human serum sample collected from a healthy man. The blood was allowed to clot and the clot was removed through centrifugation for 15 min at speed of 2000 × *g*. The serum sample separated as clear supernatant was stored at –20 °C. 2 mL of the serum was diluted to 10 mL by adding phosphate buffer (pH 7). The concentration of glucose present in serum was predetermined to be 4.98 mM by photometric sensor (Roche Cobas *c* 111 analyzer). The concentration of glucose present in serum was determined to be 5.16 mM (R.S.D = 2.47, 3 measurements) by GR-MWNTs/AuNPs/GOx film modified electrode. The concentration measured by our biosensor is in good agreement with commercial sensor certifying the accuracy of the developed modified electrode. Therefore, the biosensor holds great promise for the determination of glucose present in clinical samples.

4. Conclusions

In summary, we successfully prepared GR-MWNTs/AuNPs film and characterized by various analytical, spectral and electrochemical methods. GOx was successfully immoblized at this film. The value of Γ and k_s were estimated to be 10.51×10^{-10} mol cm^{-2} and 3.36 s^{-1}, respectively, which were significantly higher than the previous reports. The glucose biosensor detects glucose via GOx mediated oxidation and exhibits excellent electrocatalytic parameters. Two linear ranges were observed; (1) 10 μM–2 mM with LOD and sensitivity of 4.1 μM and 0.695 μA mM^{-1} cm^{-2}, respectively, (2) 2 mM–5.2 mM with LOD and sensitivity of 0.95 mM and 0.2380 μA mM^{-1} cm^{-2}. The analytical parameters were quite comparable to the previous reports. The accurate determina-

tion of glucose present in human serum sample, revealed its promising practicality. The biosensor attained appreciable stability, repeatability, and reproducibility. The simple preparation protocols, biocompatibility and electrocatalytic ability of the electrode revealed its potential applications in immobilization of enzymes and fabrication of biosensors.

Acknowledgement

This work was supported by the Ministry of Science and Technology, Taiwan (Republic of China) (NSC 103-2811-M-027-002 and 102-2113-M-027-002-MY3).

Appendix A. Supplementary data

Supplementary data associated with this article can be found, in the online version, at http://dx.doi.org/10.1016/j.enzmictec.2015.06.006

References

[1] R.R. Holman, S.K. Paul, M.A. Bethel, D.R. Matthews, H.A.W. Neil, 10-year follow-up of intensive glucose control in type 2 diabetes, N. Engl. J. Med. 359 (2008) 1577–1589.
[2] J. Wang, Glucose biosensors: 40 years of advances and challenges, Electroanalysis 13 (2001) 983.
[3] V. Mani, B. Devadas, S.-M. Chen, Direct electrochemistry of glucose oxidase at electrochemically reduced graphene oxide-multiwalled carbon nanotubes hybrid material modified electrode for glucose biosensor, Biosens. Bioelectron. 41 (2013) 309–315.
[4] S. Wang, Q. Zhang, R. Wang, S. Yoon, J. Ahn, D. Yang, et al., Multi-walled carbon nanotubes for the immobilization of enzyme in glucose biosensors, Electrochem. Commun. 5 (2003) 800–803.
[5] Wang J. Electrochemical glucose biosensors. Chemical reviews. 2008;108:814-25.
[6] B. Unnikrishnan, S. Palanisamy, S.-M. Chen, A simple electrochemical approach to fabricate a glucose biosensor based on graphene–glucose oxidase biocomposite, Biosens. Bioelectron. 39 (2013) 70–75.
[7] I. Willner, E. Katz, Integration of layered redox proteins and conductive supports for bioelectronic applications, Angew. Chem. Int. Ed. 39 (2000) 1180–1218.
[8] A.P. Periasamy, Y.-J. Chang, S.-M. Chen, Amperometric glucose sensor based on glucose oxidase immobilized on gelatin-multiwalled carbon nanotube modified glassy carbon electrode, Bioelectrochemistry 80 (2011) 114–120.
[9] N.C. Foulds, C.R. Lowe, Enzyme entrapment in electrically conducting polymers. Immobilisation of glucose oxidase in polypyrrole and its application in amperometric glucose sensors, J. Chem. Soc. Faraday Trans. 1 F 82 (1986) 1259–1264.
[10] S.A. Yamanaka, F. Nishida, L.M. Ellerby, C.R. Nishida, B. Dunn, J.S. Valentine, et al., Enzymatic activity of glucose oxidase encapsulated in transparent glass by the sol–gel method, Chem. Mater. 4 (1992) 495–497.
[11] Y. Wang, F. Caruso, Mesoporous silica spheres as supports for enzyme immobilization and encapsulation, Chem. Mater. 17 (2005) 953–961.
[12] R.B. Rakhi, K. Sethupathi, S. Ramaprabhu, A glucose biosensor based on deposition of glucose oxidase onto crystalline gold nanoparticle modified carbon nanotube electrode, J. Phy. Chem. B 113 (2009) 3190–3194.
[13] Y. Liu, M. Wang, F. Zhao, Z. Xu, S. Dong, The direct electron transfer of glucose oxidase and glucose biosensor based on carbon nanotubes/chitosan matrix, Biosens. Bioelectron. 21 (2005) 984–988.
[14] S. Yang, Z. Lu, S. Luo, C. Liu, Y. Tang, Direct electrodeposition of a biocomposite consisting of reduced graphene oxide, chitosan and glucose oxidase on a glassy carbon electrode for direct sensing of glucose, Microchim. Acta 180 (2013) 127–135.
[15] Q. Chang, H. Tang, Optical determination of glucose and hydrogen peroxide using a nanocomposite prepared from glucose oxidase and magnetite nanoparticles immobilized on graphene oxide, Microchim. Acta 181 (2014) 527–534.
[16] V. Mani, R. Devasenathipathy, S.-M. Chen, S.-T. Huang, V. Vasantha, Immobilization of glucose oxidase on graphene and cobalt phthalocyanine composite and its application for the determination of glucose, Enzyme Microb. Technol. 66 (2014) 60–66.
[17] B. Devadas, V. Mani, S.-M. Chen, A glucose/O_2 biofuel cell based on graphene and multiwalled carbon nanotube composite modified electrode, Int. J. Electrochem. Sci. 7 (2012) 8064–8075.
[18] S. Palanisamy, C. Karuppiah, Chen S-M. Direct electrochemistry and electrocatalysis of glucose oxidase immobilized on reduced graphene oxide and silver nanoparticles nanocomposite modified electrode, Colloids Surf. B 114 (2014) 164–169.
[19] W.S. Hummers Jr, R.E. Offeman, Preparation of graphitic oxide, J. Am. Chem. Soc. 80 (1958) 1339.
[20] B. Dinesh, V. Mani, R. Saraswathi, S.-M. Chen, Direct electrochemistry of cytochrome c immobilized on a graphene oxide-carbon nanotube composite for picomolar detection of hydrogen peroxide, RSC Adv. 4 (2014) 28229–28237.
[21] R. Devasenathipathy, V. Mani, S.-M. Chen, Highly selective amperometric sensor for the trace level detection of hydrazine at bismuth nanoparticles decorated graphene nanosheets modified electrode, Talanta 124 (2014) 43–51.
[22] V. Mani, S.-M. Chen, B.-S. Lou, Three dimensional graphene oxide-carbon nanotubes and graphene-carbon nanotubes hybrids, Int. J. Electrochem. Sci. 8 (2013) 11641–11660.
[23] V.K. Ponnusamy, V. Mani, S.-M. Chen, W.-T. Huang, J. Jen, Rapid microwave assisted synthesis of graphene nanosheets/polyethyleneimine/gold nanoparticle composite and its application to the selective electrochemical determination of dopamine, Talanta 120 (2014) 148–157.
[24] A.J. Bard, L.R. Faulkner, Electrochemical Methods: Fundamentals and Applications, Wiley New York, 1980.
[25] C. Deng, J. Chen, X. Chen, C. Xiao, L. Nie, S. Yao, Direct electrochemistry of glucose oxidase and biosensing for glucose based on boron-doped carbon nanotubes modified electrode, Biosens. Bioelectron. 23 (2008) 1272–1277.
[26] X. Kang, J. Wang, H. Wu, I.A. Aksay, J. Liu, Y. Lin, Glucose oxidase–graphene–chitosan modified electrode for direct electrochemistry and glucose sensing, Biosens. Bioelectron. 25 (2009) 901–905.
[27] H. Zhang, Z. Meng, Q. Wang, J. Zheng, A novel glucose biosensor based on direct electrochemistry of glucose oxidase incorporated in biomediated gold nanoparticles–carbon nanotubes composite film, Sens. Actuators, B 158 (2011) 23–27.
[28] X. Luo, A.J. Killard, M.R. Smyth, Reagentless glucose biosensor based on the direct electrochemistry of glucose oxidase on carbon nanotube-modified electrodes, Electroanalysis 18 (2006) 1131–1134.
[29] Y. Zhou, H. Yang, H.-Y. Chen, Direct electrochemistry and reagentless biosensing of glucose oxidase immobilized on chitosan wrapped single-walled carbon nanotubes, Talanta 76 (2008) 419–423.
[30] K.-Y. Hwa, B. Subramani, Synthesis of zinc oxide nanoparticles on graphene-carbon nanotube hybrid for glucose biosensor applications, Biosens. Bioelectron. 62 (2014) 127–133.